O, wonder!
How many goodly creatures are there here!
How beauteous mankind is! O brave new world,
That has such people in't.
William Shakespeare, *The Tempest*, c. 1611.

CHAPTER 12

Geostrophic Turbulence and Baroclinic Eddies

GEOSTROPHIC TURBULENCE is turbulence in flows that are stably stratified and close to geostrophic balance. Like most aspects of turbulence the subject is difficult, and a real 'solution' — meaning an accurate, informative statement about average states, without computation of the detailed evolution — may be out of our reach, and may not exist. Ironically, it is sometimes easier to say something interesting about geostrophic turbulence than about incompressible isotropic two- or three-dimensional turbulence. In the latter class of problems there is nothing else to understand other than the problem of turbulence itself, and this is like climbing a smooth marble wall. On the other hand, rotation and stratification give one something else to grasp, a thorn though it may be, and it becomes possible to address geophysically interesting phenomena without having to solve the whole turbulence problem. Furthermore, in inhomogeneous geostrophic turbulence, asking questions about the *mean fields* is meaningful and useful, whereas this is uninteresting in isotropic turbulence.

The subject of geostrophic turbulence is a wondrous one, giving rise to phenomena that are both beautiful and important — the jets and eddies on Jupiter and the weather on Earth are but two examples. The subject is not restricted to quasi-geostrophic flow, and the large scale turbulence of Earth's ocean and atmosphere is sometimes simply called 'macro-turbulence'. Nevertheless, the quasi-geostrophic equations describe the main effects: they retain advective nonlinearity in the vorticity equation, and they capture the constraining effects of rotation and stratification that are so important in geophysical flows in a simple and direct way; for these reasons the quasi-geostrophic equations will be our main tool. Let us consider the effects of rotation first, then stratification.

12.1 DIFFERENTIAL ROTATION IN TWO-DIMENSIONAL TURBULENCE

In the limit of motion of a scale much shorter than the deformation radius, and with no topography, the quasi-geostrophic potential vorticity equation, (5.118), reduces to the two-dimensional equation,

$$\frac{\mathrm{D}q}{\mathrm{D}t} = 0, \tag{12.1}$$

where $q = \zeta + f$. This is the perhaps the simplest equation with which to study the effects of rotation on turbulence. Suppose first that the Coriolis parameter is constant, so that $f = f_0$. Then (12.1)

becomes simply the two-dimensional vorticity equation

$$\frac{\mathrm{D}\zeta}{\mathrm{D}t} = 0. \tag{12.2}$$

Thus constant rotation has *no* effect on purely two-dimensional motion. Flow that is already two-dimensional — flow on a soap film, for example — is unaffected by rotation. (In the ocean and atmosphere, or in a rotating tank, it is of course the effects of rotation that lead to the flow being quasi-two dimensional in the first instance.)

Suppose, though, that the Coriolis parameter is variable, as in $f = f_0 + \beta y$. Then we have

$$\frac{\mathrm{D}}{\mathrm{D}t}(\zeta + \beta y) = 0 \qquad \text{or} \qquad \frac{\mathrm{D}\zeta}{\mathrm{D}t} + \beta v = 0. \tag{12.3a,b}$$

If the asymptotically dominant term in these equations is the one involving β then we must have $v = 0$ at lowest order. That is, if β is very large, then the meridional flow v must be correspondingly small to ensure that the equation can balance, and this argument holds in the presence of forcing and dissipation. Any flow must then be predominantly *zonal*. A closely related argument uses the conservation of angular momentum as follows. A ring of fluid encircling the Earth at a velocity u has an angular momentum per unit mass $a\cos\vartheta(u + \Omega a\cos\vartheta)$, where ϑ is the latitude and a is the radius of the Earth. Moving this ring of air polewards while conserving its angular momentum requires that its zonal velocity and hence energy must increase, so unless there is a source for that energy the flow is constrained to remain zonal.

In the following sections we look at the mechanism of jet formation in a little more detail. We first give some fairly general scaling arguments, and then proceed in two complementary ways — first with an argument couched in spectral space using the language of turbulent cascades, and second with an argument in physical space. In Section 15.1 we come back to the problem from a third perspective, one particularly appropriate for Earth's atmosphere.

12.1.1 The Wave–Turbulence Cross-over

Scaling

Let us now consider how turbulent flow might interact with Rossby waves. We write (12.1) in full as

$$\frac{\partial\zeta}{\partial t} + \boldsymbol{u}\cdot\nabla\zeta + \beta v \;\; = 0. \tag{12.4}$$

If $\zeta \sim U/L$ and if $t \sim T$ then the respective terms in this equation scale as

$$\frac{U}{LT} \qquad \frac{U^2}{L^2} \qquad \beta U. \tag{12.5}$$

The way that time scales (i.e., advectively or with a Rossby wave frequency scaling) is determined by which of the other two terms dominates, and this in turn is scale dependent. For large scales the β-term is dominant, and at smaller scales the advective term is dominant. The cross-over scale, denoted L_R, is called the *Rhines scale* and is given by[1]

$$L_R \sim \left(\frac{U}{\beta}\right)^{1/2}. \tag{12.6}$$

The U in (12.6) should be interpreted as the root-mean-square velocity at the energy containing scales, not a mean or translational velocity. We refer to the specific scale $\sqrt{U/\beta}$ as the Rhines scale,

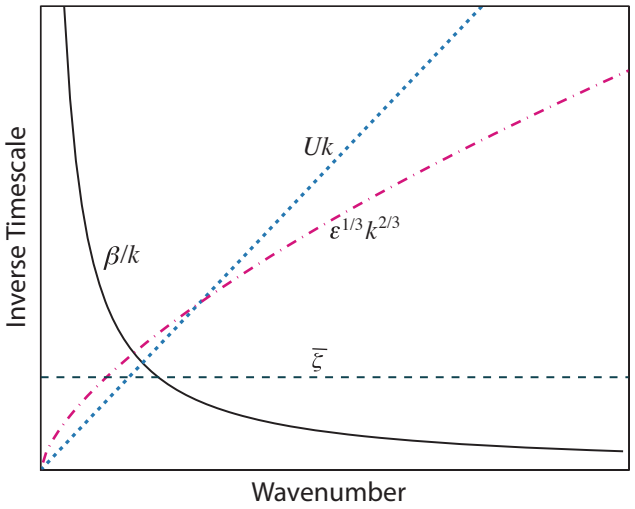

Fig. 12.1 Inverse timescales, or frequencies, in wavenumber space in beta-plane turbulence. The solid curve is the frequency of Rossby waves, proportional to β/k, and the other three curves are various estimates of the inverse turbulence time scale. These are the turbulent eddy transfer rate, proportional to $\varepsilon^{1/3}k^{2/3}$ in a $k^{-5/3}$ spectrum; the estimate Uk where U is a root-mean-squared velocity; and the mean vorticity, which is constant.

Where the Rossby wave frequency is larger (smaller) than the turbulent frequency, i.e., at large (small) scales, Rossby waves (turbulence) dominate the dynamics.

L_R, and more general scales involving a balance between nonlinearity and β as the β-scale, denoted L_β.

This is not a unique way to arrive at a β-scale, since we have chosen the length scale that connects vorticity to velocity to also be the β-scale, and it is not obvious that this should be so. If the two scales are different, the three terms in (12.4) scale as

$$\frac{\mathcal{Z}}{T} \qquad \frac{U\mathcal{Z}}{L} \qquad \beta U, \tag{12.7}$$

respectively, where $\mathcal{Z}$ is the scaling for vorticity; that is, $\zeta = \mathcal{O}(\mathcal{Z})$. Equating the second and third terms gives the scale

$$L_{\beta\mathcal{Z}} = \frac{\mathcal{Z}}{\beta}. \tag{12.8}$$

Although (12.6) and (12.8) differ in detail, both indicate that at some *large* scale Rossby waves are likely to dominate whereas at small scales advection and turbulence dominate.

Another heuristic way to derive (12.6) is by a direct consideration of time scales. Ignoring anisotropy, Rossby wave frequency is β/k and an inverse advective time scale is Uk, where k is the wavenumber. Equating these two gives an equation for the Rhines wavenumber

$$k_R \sim \left(\frac{\beta}{U}\right)^{1/2}. \tag{12.9}$$

This equation is the inverse of (12.6), but factors of order unity (e.g., π) cannot be revealed by simple scaling arguments such as these. We denote the Rhines wavenumber as k_R and a more generic cross-over wavenumber as k_β (and below we also introduce k_ε). The cross-over between waves and turbulence is reasonably sharp, as indicated in Fig. 12.1.

Turbulent phenomenology

We now examine wave–turbulence cross-over using the phenomenology of two-dimensional turbulence. We will suppose that the fluid is stirred at some well-defined scale k_f, producing an energy input ε. Then (assuming no energy is lost to smaller scales) energy cascades to large scales at that same rate. At some scale, the β-term in the vorticity equation will start to make its presence felt. By analogy with the procedure for finding the viscous dissipation scale in turbulence, we can find the

scale at which linear Rossby waves dominate by equating the inverse of the turbulent eddy turnover time to the Rossby wave frequency. The eddy-turnover time is

$$\tau_k = \varepsilon^{-1/3} k^{-2/3}, \tag{12.10}$$

and equating this to the inverse Rossby wave frequency k/β gives estimates for the β-wavenumber and its inverse, the β-scale, namely

$$k_\varepsilon = \left(\frac{\beta^3}{\varepsilon}\right)^{1/5}, \qquad L_\varepsilon = \left(\frac{\varepsilon}{\beta^3}\right)^{1/5}. \tag{12.11a,b}$$

We denote these scales with a subscript ε because of the appearance of the energy cascade rate. In a real fluid these expressions are harder to evaluate than (12.9), since it is generally much easier to measure velocities than energy transfer rates, or even vorticity. On the other hand, (12.11) is more satisfactory from the point of view of turbulence theory because ε may be determined by processes largely independent of β, whereas the magnitude of the eddies at the energy containing scales is likely to be a function of β. We also remark that the scale given by (12.11b) is not necessarily the energy-containing scale, and may in principle differ considerably from the scale given by (12.9). This is because the inverse cascade is not necessarily *halted* at the scale (12.11b) — this is just the scale at which Rossby waves become important. Energy may continue to cascade to larger scales, albeit anisotropically as discussed below, and so the energy containing scale may be larger.

12.1.2 Generation of Zonal Flows and Jets

None of the effects discussed so far takes into account the anisotropy inherent in Rossby waves, and such anisotropy can give rise to predominantly zonal flows and jets. To understand this, let us first note that energy transfer will be relatively inefficient at those scales where linear Rossby waves dominate the dynamics. But the wave–turbulence boundary is not isotropic; the Rossby wave frequency is quite anisotropic, being given by

$$\omega = -\frac{\beta k^x}{k^{x2} + k^{y2}}. \tag{12.12}$$

If, albeit a little crudely, we suppose that the turbulent part of the flow remains isotropic, the wave–turbulence boundary is then given by equating the inverse of (12.10) with (12.12) and is a solution of

$$\varepsilon^{1/3} k^{2/3} = \frac{\beta k^x}{k^2}, \tag{12.13}$$

where k is the isotropic wavenumber. Solving this gives expressions for the x- and y-wavenumber components of the wave–turbulence boundary, namely

$$k^x_\varepsilon = \left(\frac{\beta^3}{\varepsilon}\right)^{1/5} \cos^{8/5}\theta, \qquad k^y_\varepsilon = \left(\frac{\beta^3}{\varepsilon}\right)^{1/5} \sin\theta \cos^{3/5}\theta, \tag{12.14}$$

where the polar coordinate is parameterized by the angle $\theta = \tan^{-1}(k^y/k^x)$. This odd-looking formula is illustrated in Fig. 12.2, and it defines the anisotropic wave-turbulence boundary. (Slight variations on this theme are produced by using different expressions for the turbulence time scale.)

What occurs physically? The region inside the dumbbell shapes in Fig. 12.2 is dominated by Rossby waves, where the natural frequency of the oscillation is *higher* than the turbulent frequency. If the flow is stirred at a wavenumber higher than this the energy will cascade to larger scales, but because of the frequency mismatch the turbulent flow will be unable to efficiently excite modes within the dumbbell. Nevertheless, there is still a natural tendency of the energy to seek the gravest

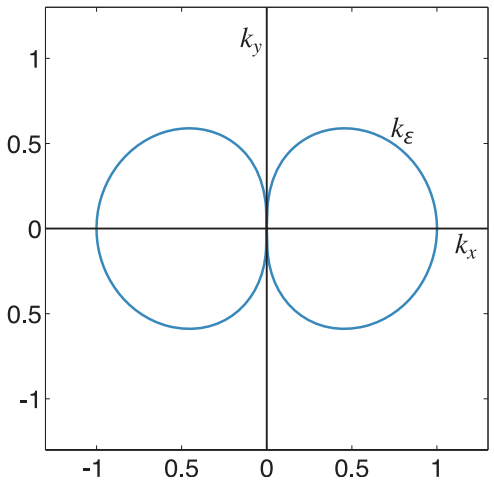

Fig. 12.2 The anisotropic wave–turbulence boundary k_ε, in wave-vector space calculated by equating the turbulent eddy transfer rate, proportional to $k^{2/3}$ in a $k^{-5/3}$ spectrum, to the Rossby wave frequency $\beta k^x/k^2$, as in (12.14).The wavenumbers are scaled such that $\beta^3/\varepsilon = 1$.

Within the dumbbell Rossby waves dominate and energy transfer is inhibited. The inverse cascade plus Rossby waves thus leads to a generation of zonal flow.

mode, and it will do this by cascading toward the $k^x = 0$ axis; that is, toward zonal flow. Thus, the combination of Rossby waves and turbulence will lead to the formation of zonal flow and, potentially, zonal jets.[3]

Figure 12.3 illustrates this mechanism; it shows the freely evolving (unforced, inviscid) energy spectrum in a simulation on a β–plane, with an initially isotropic spectrum. The energy implodes, cascading to larger scales but avoiding the region inside the dumbbell and piling up at $k^x = 0$. In physical space the flow organizes itself into zonally elongated structures and jets, in both freely-decaying and forced-dissipative simulations (Fig. 12.4 and Fig. 12.7).

† *Joint effect of beta and friction*

The β term does not remove energy from a fluid. Thus, if energy is being added to a fluid at some small scales, and the energy is cascading to larger scales, then the β-effect does not of itself halt the inverse cascade, it merely deflects the cascade such that the flow becomes more zonal. Suppose that the fluid obeys the barotropic vorticity equation,

$$\frac{\partial \zeta}{\partial t} + J(\psi, \zeta) + \beta \frac{\partial \psi}{\partial x} = F - r\zeta + \nu \nabla^2 \zeta, \tag{12.15}$$

where the viscosity, ν, is small and acts only to remove enstrophy, and not energy, at very small scales. The forcing, F, supplies energy at a rate ε and this is cascaded upscale and removed by the linear drag term $-r\zeta$, where the drag coefficient r is a constant. If the friction is sufficiently large then the energy is removed before it feels the effect of β at the scale (11.68), namely $L_r = (\varepsilon/r^3)^{1/2}$. However, if friction is small, such that $L_\varepsilon = (\varepsilon/\beta^3)^{1/5}$ is smaller than L_r, then the cascade feels the beta effect before it feels frictional effects, and L_r is then unlikely to be a relevant parameter.

If the forcing scale is small and an inverse cascade exists, the turbulence is characterized by three parameters, β, ε and r. There is only one way to make a nondimensional parameter from these and this is

$$\gamma = \beta^2 \epsilon r^{-5}, \tag{12.16}$$

along with powers of γ. There is no unique way to make a length scale from these parameters, but various scales arise phenomenologically. One is L_ε, noted above, and another arises from energetic considerations. If we form an energy equation from (12.15) by multiplying by $-\psi$ and spatially integrating (and neglecting viscosity) we find the energy balance

$$\varepsilon = -\frac{1}{A}\int_A \psi F \, \mathrm{d}A = \frac{r}{A}\int_A (\nabla\psi)^2 \, \mathrm{d}A = 2r\overline{E}, \tag{12.17}$$

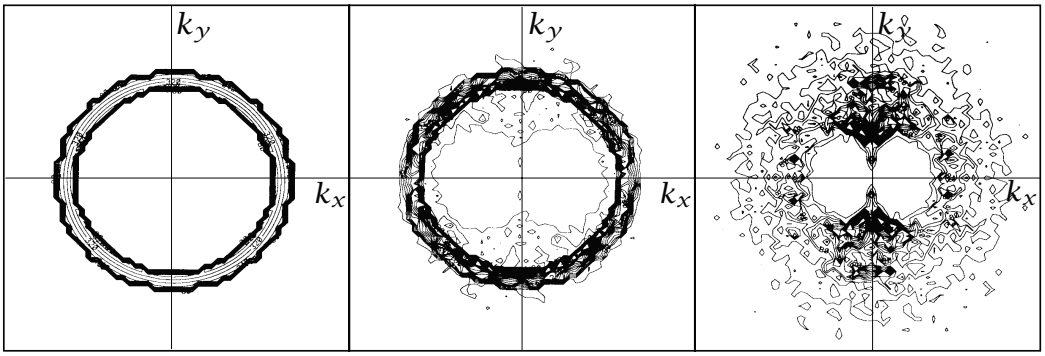

Fig. 12.3 Evolution of the energy spectrum in a freely evolving two-dimensional simulation on the β-plane. The panels show contours of energy in wavenumber (k_x, k_y) space at successive times. The initial spectrum is isotropic. The energy 'implodes', but its passage to large scales is impeded by the β-effect, and the second and third panels show the spectrum at later times, illustrating the dumbbell predicted by (12.14) and Fig. 12.2.[2]

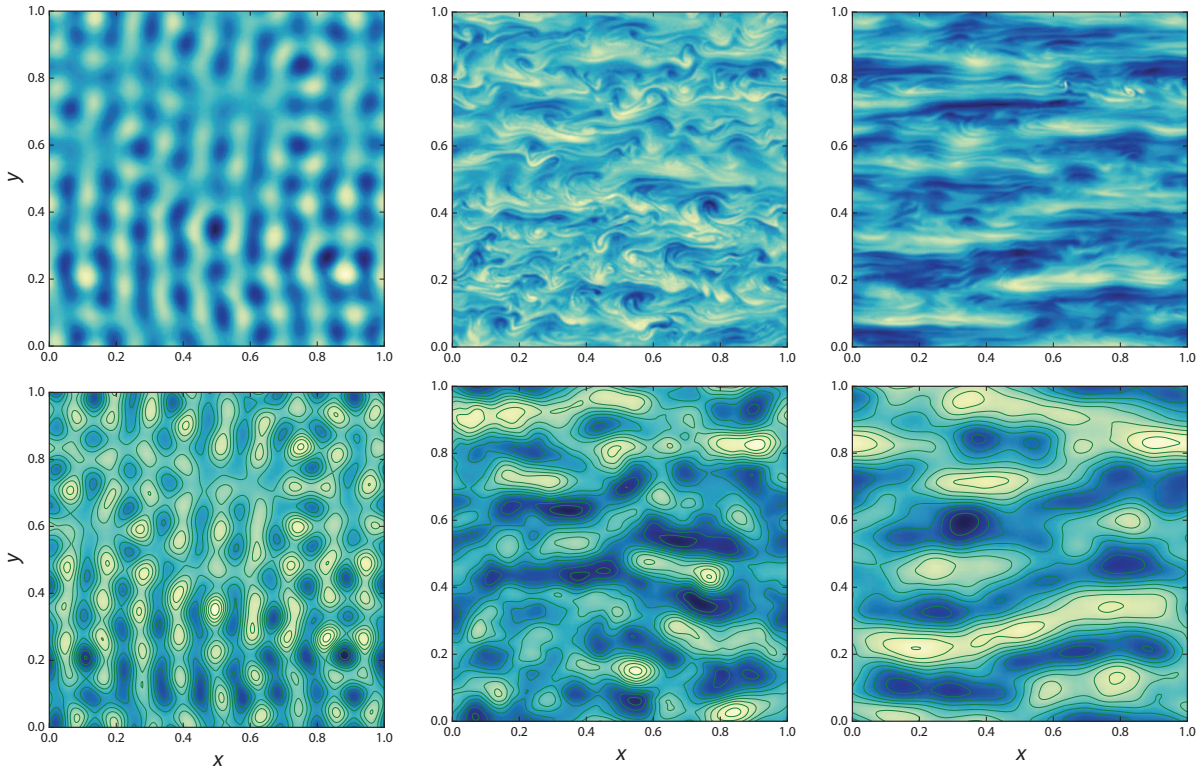

Fig. 12.4 Evolution of vorticity (top) and streamfunction (bottom) in a doubly periodic domain on the β-plane, obeying (12.4) with the addition of a weak viscous term on the right-hand side. The initial conditions are the same as for Fig. 11.8, and time proceeds from left to right. Compared to Fig. 11.8, vortex formation is inhibited and there is a tendency toward zonal flow.

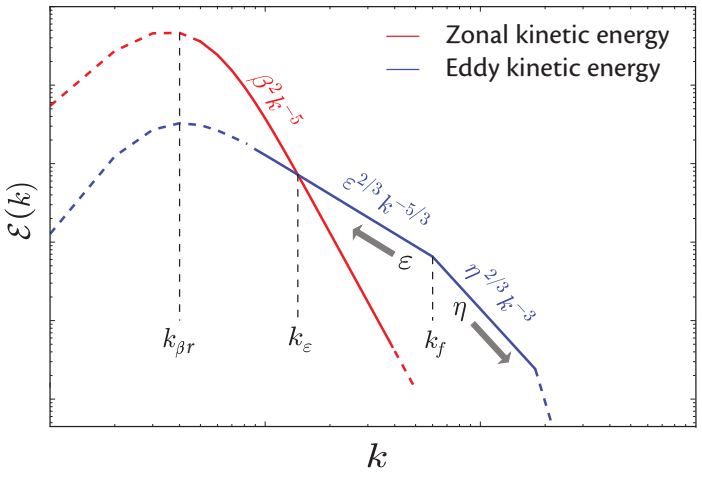

Fig. 12.5 Putative kinetic spectra, $\mathcal{E}(k)$, in beta-plane turbulence. Energy injected at wavenumber k_f cascades to larger scales until it reaches the turbulent beta scale, k_ε. The energy in the zonal modes then forms a zonostrophic k^{-5} spectrum which extends as far as the frictional Rhines scale, $k_{\beta r}$.

where $\overline{E}$ is the average energy of the fluid per unit mass. This expression holds whether or not β is non-zero. Using (12.6) with $U = \sqrt{2\overline{E}}$, where $\overline{E}$ is obtained from (12.17), we obtain the scale

$$L_{\beta r} = \left(\frac{\varepsilon}{r\beta^2}\right)^{1/4}, \tag{12.18}$$

which may be thought of as a prediction for the Rhines scale, L_R. The ratio of the scales $L_{\beta r}$ to L_ε is

$$\frac{L_{\beta r}}{L_\varepsilon} = \left(\frac{\beta^2\varepsilon}{r^5}\right)^{1/20} = \gamma^{1/20}. \tag{12.19}$$

What do the two scales, L_ε and $L_{\beta r}$, represent? The first is the scale at which the β-effect is first felt by the inverse cascade, and it is relevant for large-scale meridional mixing, and so for the meridional heat transport in the atmosphere. If friction is small (i.e., if $\gamma \gg 1$) the inverse energy transfer will continue past this scale, with the energy largely being at very small values of k_x, and (12.18) then characterizes the largest scale reached by the inverse cascade, and so the meridional scale of the jets. In this region one might hypothesize that the spectrum is determined by β and k alone, and if so it is given by

$$\mathcal{E}(k) = \mathcal{C}_z\beta^2 k^{-5}, \tag{12.20}$$

where $\mathcal{C}_z$ is a constant, and most of the energy is in the zonal flow. Only the extent (and not the amplitude) of this region is then determined by the forcing strength. Turbulence of this character is called *zonostrophic,* and is illustrated in Fig. 12.5. However, we might also expect the drag coefficient, r, to be a factor in at least part of spectral slope because, with such a steep slope, the timescale of the flow diminishes as the wavenumber falls, so there is no scale, L_{fric} say, such that friction acts only at scales larger than it.[4] But rather than pursuing more arguments in spectral space, let us turn to a physical space argument.

12.1.3 Potential Vorticity Staircases

Let us now consider a complimentary approach in physical space, with the essential idea being the following. Suppose that a turbulent flow exists on a background state that has a potential vorticity gradient, such as might be caused by the beta-effect. The eddies will seek to homogenize the potential vorticity but, in general, they will be unable to do so completely. Instead, the flow becomes partially homogenized, with regions of homogeneous potential vorticity separated by jumps, as

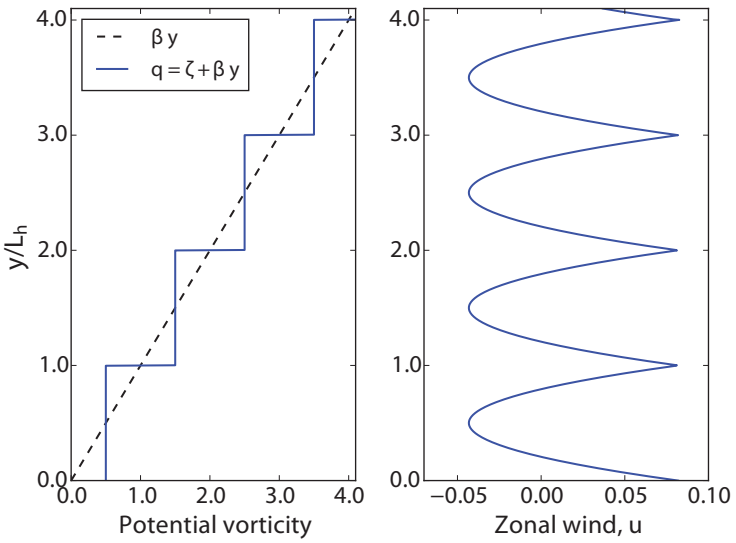

Fig. 12.6 An idealized potential vorticity staircase on a β-plane with $\beta = 1$. The left panel shows homogeneous regions of potential vorticity of meridional extent L_h separated by jumps, as calculated using (12.24). The right-hand panel shows the corresponding zonal flow, calculated using (12.28) with u_0 chosen to be such that the average zonal flow is zero.

illustrated in Fig. 12.6. Such a structure is called a *potential vorticity staircase,* and the staircase implies the existence of zonal jets.[5]

The homogenization of a scalar is discussed further in Section 13.5, but it can be imagined that, in a turbulent flow, the gradients of a scalar that is both advected and diffused will become smeared out as much as possible: diffusion will dissipate any extrema and advection cannot recreate them. Potential vorticity is a scalar, so we might expect it too to become homogenized, but it is not passive and therefore the process of homogenization will affect the flow itself, preventing complete homogenization. One reason for that may be the boundary conditions, another that the process of homogenization requires more energy than the flow contains. To see this, consider a freely-evolving flow on a beta-plane obeying the barotropic vorticity equation

$$\frac{\partial \zeta}{\partial t} + J(\psi, \zeta + \beta y) = \nu \nabla^2 \zeta, \tag{12.21}$$

where ν is sufficiently small that energy is well conserved over the timescales of interest. If potential vorticity, $q = \zeta + \beta y$, is to be homogenized over some meridional scale L then, in the homogenized region, $\zeta \approx -\beta y$. If the flow is predominantly zonal then this gives the estimate $U \sim \beta y^2$ and the energy in the region is, very approximately,

$$\frac{1}{2} \int u^2 \, \mathrm{d}x \, \mathrm{d}y \approx \int (\beta y^2)^2 \, \mathrm{d}x \, \mathrm{d}y, \tag{12.22}$$

giving the estimate $U^2 L \sim \beta^2 L^5$. If we suppose that the initial root-mean square velocity is also U, and that the flow becomes predominantly zonal, then solving the above estimate for L suggests that the potential vorticity will become homogenized over the scale

$$L_h \sim \left(\frac{U}{\beta} \right)^{1/2}. \tag{12.23}$$

This is the same as the Rhines scale given in (12.6), as it has to be by dimensional analysis, although now it is supposed that much of the energy lies in the zonal flow. Although the scale is the same, this way of looking at the problem adds something to the physical picture — *an asymmetry between eastward and westward flow,* as we now discuss.

In the idealized staircase of Fig. 12.6 potential vorticity is piecewise continuous and given by

$$q = \zeta + \beta y = q_0, \qquad 0 < y < L_h, \tag{12.24a}$$

$$q = \zeta + \beta y = q_0 + \beta L_h \equiv q_1, \qquad L_h < y < 2L_h, \quad \text{and so on.} \tag{12.24b}$$

In any one of the homogenized regions the flow is given by solving

$$\frac{\partial u}{\partial y} = \beta y - q_n \quad \text{giving} \quad u = \frac{1}{2}\beta y^2 - q_n y + \text{constant}, \tag{12.25}$$

where $q_n = \beta L_h/2 + n\beta L_h$. The constant may be determined by requiring continuity of u across the regions, and we then obtain

$$u = \frac{1}{2}\beta(y - L_h/2)^2 + u_0, \qquad 0 < y < L_h, \tag{12.26}$$

$$u = \frac{1}{2}\beta(y - 3L_h/2)^2 + u_0, \qquad L_h < y < 2L_h, \tag{12.27}$$

or in general,

$$u = \frac{1}{2}\beta\left(y - (n - 1/2)L_h\right)^2 + u_0, \qquad (n-1)L_h < y < nL_h, \qquad n = 1, 2, 3 \ldots , \tag{12.28}$$

where u_0 is a constant. Relative to u_0, the flow is weakly westward in the homogenized regions, whereas in the transition region the flow has a sharp eastward peak, as shown in Fig. 12.6. The spectrum of such a flow is k^{-4}, similar to the k^{-5} spectrum of zonostrophic flow.

Finally, let us make a few remarks. First, the potential vorticity gradient does not change sign, so the flow is (just) barotropically stable — one is supposing that the eddies arise by some external mechanism (e.g., some external stirring, or baroclinic instability) and they are creating the jet, not vice versa. Second, the staircase structure implies that potential vorticity is (obviously) well mixed in the regions of constant potential vorticity, but that there is no mixing across the jumps. The jumps are known as *mixing barriers* and, once formed, are found to be very persistent in numerical simulations. The edge of the stratospheric polar vortex, and the boundaries of ocean gyres, may also be examples. A fluid parcel is energetically incapable of jumping across the barrier, and the barrier's existence makes clear that parameterizing turbulent mixing as a downgradient flux of a conserved quantity cannot always work, at least with a constant diffusivity, since here the gradient is strong but the mixing is weak.

Numerical simulations do reproduce the staircase in some, but not all, circumstances (Fig. 12.7). The simulations suggest that there needs to be a good separation between the turbulent beta scale and the Rhines scales, in particular with $L_R/L_\epsilon \gg 1$, and that this is best achieved with weak friction and/or forcing that is at large scales, perhaps even larger than L_ϵ. However, the subject continues to evolve and the reader should consult the primary literature to learn more.

12.1.4 † Zonal Jets — Other Mechanisms and Final Remarks

In the above we have described how zonal jets may be created from two distinct points of view — one in spectral space and the other in physical space. We described the spectral approach in terms of a cascade — a local energy transfer from one wavenumber to another. However, in many circumstances the energy transfer from eddies to zonal flow may be much more direct, with no spectral intermediaries. That is, a zonally asymmetric flow may be unstable and, even in the absence of eddy-eddy interactions, produce a zonal jet. The interaction is then deemed 'quasi-linear' and the triad interaction is highly nonlocal, as in the right-hand panel of Fig. 11.1. There are still other ways in which we may describe jet formation, some described in section 15.1. It is the parameters of the problem at hand that will determine which mechanism is dominant in a particular situation, although a full understanding of their similarities and differences remains tenebrous.[7]

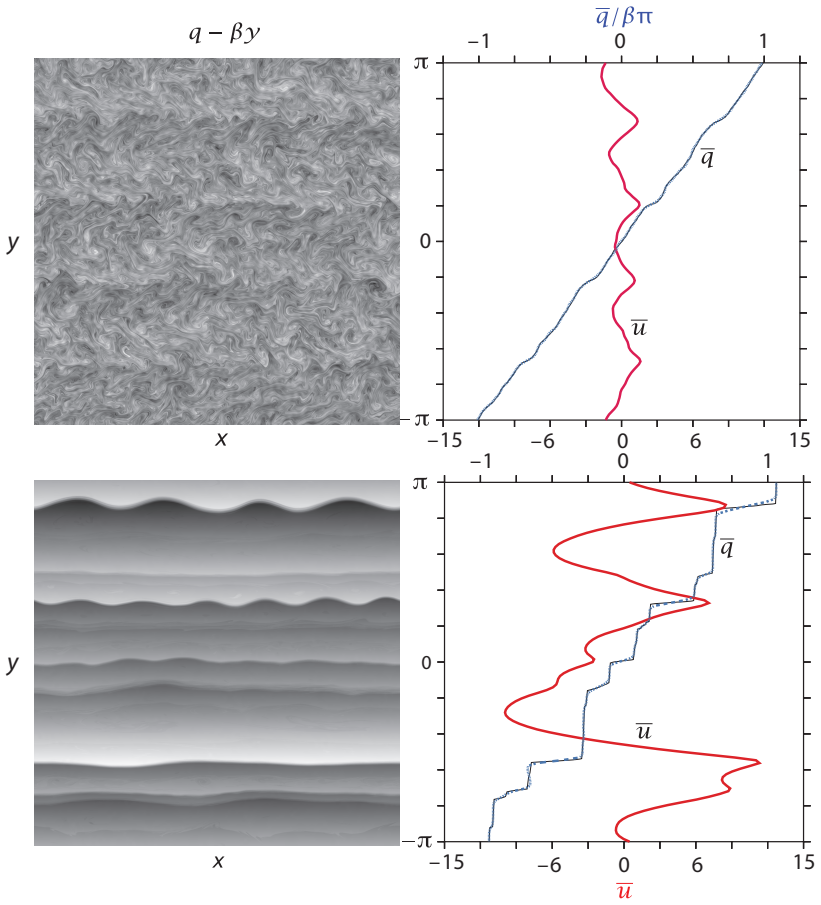

Fig. 12.7 Simulations of two-dimensional turbulence on a beta-plane.[6]

The left panels show snapshots of the relative vorticity ζ, and right panels show zonally-averaged potential vorticity and zonal wind. The top panels show an integration with $L_R/L_\varepsilon \approx 3$ and the bottom panels have $L_R/L_\varepsilon \approx 11$.

12.2 STRATIFIED GEOSTROPHIC TURBULENCE

12.2.1 An Analogue to Two-dimensional Flow

Now let us consider stratified effects in a simple setting, using the quasi-geostrophic equations with constant Coriolis parameter and constant stratification.[8] The (dimensional) unforced and inviscid governing equation may then be written as

$$\frac{\mathrm{D}q}{\mathrm{D}t} = 0, \qquad q = \nabla^2\psi + Pr^2\frac{\partial^2\psi}{\partial z^2}, \tag{12.29a}$$

where $Pr = f_0/N$ is the *Prandtl ratio* (and Pr/H is the inverse of the deformation radius) and $\mathrm{D}/\mathrm{D}t = \partial/\partial t + \boldsymbol{u}\cdot\nabla$ is the two-dimensional material derivative. The vertical boundary conditions are

$$\frac{\mathrm{D}}{\mathrm{D}t}\left(\frac{\partial\psi}{\partial z}\right) = 0, \qquad \text{at } z = 0, H. \tag{12.29b}$$

These equations are analogous to the equations of motion for purely two-dimensional flow. In particular, with periodic lateral boundary conditions, or conditions of no-normal flow, there are two quadratic invariants of the motion, the energy and the enstrophy, which are obtained by multiplying (12.29a) by $-\psi$ and q and integrating over the domain, as in Chapter 5. The conserved energy is

$$\frac{\mathrm{d}\widehat{E}}{\mathrm{d}t} = 0, \qquad \widehat{E} = \frac{1}{2}\int_V \left[(\nabla\psi)^2 + Pr^2\left(\frac{\partial\psi}{\partial z}\right)^2\right]\mathrm{d}V, \tag{12.30}$$

where the integral is over a *three-dimensional* domain. The enstrophy is conserved at each vertical level, and of course the volume integral is also conserved, namely

$$\frac{\mathrm{d}\widehat{Z}}{\mathrm{d}t} = 0, \qquad \widehat{Z} = \frac{1}{2}\int_V q^2\,\mathrm{d}V = \frac{1}{2}\int_V \left[\nabla^2\psi + Pr^2\left(\frac{\partial^2\psi}{\partial z^2}\right)\right]^2 \mathrm{d}V. \tag{12.31}$$

The analogy with two-dimensional flow is even more transparent if we further rescale the vertical coordinate by $1/Pr$, and so let $z' = z/Pr$. Then the energy and enstrophy invariants are:

$$\widehat{E} = \int (\nabla_3\psi)^2\,\mathrm{d}V, \qquad \widehat{Z} = \int q^2\,\mathrm{d}V = \int (\nabla_3^2\psi)^2\,\mathrm{d}V, \tag{12.32}$$

where $\nabla_3 = \mathbf{i}\partial/\partial x + \mathbf{j}\partial/\partial y + \mathbf{k}\partial/\partial z'$. The invariants then have almost the same form as the two-dimensional invariants, but with a three-dimensional Laplacian operator instead of a two-dimensional one.

Given these invariants, we should expect that any dynamical behaviour that occurs in the two-dimensional equations *that depends solely on the energy/enstrophy constraints* should have an analogue in quasi-geostrophic flow. In particular, the transfer of energy to large-scales and enstrophy to small scales will also occur in quasi-geostrophic flow with, in so far as these transfers are effected by a local cascade, corresponding spectra of $k^{-5/3}$ and k^{-3}. However, in the quasi-geostrophic case, it is the *three-dimensional* wavenumber that is relevant, with the vertical component scaled by the Prandtl ratio. As a consequence, the energy cascade to larger horizontal scales is generally accompanied by a cascade to larger vertical scales — a *barotropization* of the flow. Still, the analogy between two-dimensional and quasi-geostrophic cascades should not be taken too far, because in the latter the potential vorticity is advected only by the horizontal flow. Thus, the dynamics of quasi-geostrophic turbulence will *not* in general be isotropic in three-dimensional wavenumber. To examine these dynamics more fully we first turn to a simpler model, that of two-layer flow.

12.2.2 Two-layer Geostrophic Turbulence

Let us consider flow in two layers of equal depth, governed by the quasi-geostrophic equations with (for now) $\beta = 0$, namely

$$\frac{\partial q_i}{\partial t} + J(\psi_i, q_i) = 0, \qquad i = 1, 2, \tag{12.33}$$

where

$$q_1 = \nabla^2\psi_1 + \frac{1}{2}k_d^2(\psi_2 - \psi_1), \qquad q_2 = \nabla^2\psi_2 + \frac{1}{2}k_d^2(\psi_1 - \psi_2), \tag{12.34a}$$

$$J(a,b) = \frac{\partial a}{\partial x}\frac{\partial b}{\partial y} - \frac{\partial a}{\partial y}\frac{\partial b}{\partial x}, \qquad \frac{1}{2}k_d^2 = \frac{2f_0^2}{g'H} \equiv \frac{4f_0^2}{N^2H^2}. \tag{12.34b}$$

The wavenumber k_d is inversely proportional to the baroclinic radius of deformation, and the two equivalent expressions given are appropriate in a layered model and a level model, respectively. The equations conserve the total energy,

$$\frac{\mathrm{d}\widehat{E}}{\mathrm{d}t} = 0, \qquad \widehat{E} = \frac{1}{2}\int_A \left[(\nabla\psi_1)^2 + (\nabla\psi_2)^2 + \frac{1}{2}k_d^2(\psi_1 - \psi_2)^2\right]\mathrm{d}A, \tag{12.35}$$

and the enstrophy in each layer

$$\frac{\mathrm{d}\widehat{Z}_1}{\mathrm{d}t} = 0, \qquad \widehat{Z}_1 = \int_A q_1^2\,\mathrm{d}A, \tag{12.36a}$$

$$\frac{\mathrm{d}\widehat{Z}_2}{\mathrm{d}t} = 0, \qquad \widehat{Z}_2 = \int_A q_{12}^2 \,\mathrm{d}A. \tag{12.36b}$$

The first two terms in the energy expression, (12.35), represent the kinetic energy, and the last term is the available potential energy, proportional to the variance of temperature.

Baroclinic and barotropic decomposition

Define the barotropic and baroclinic streamfunctions by

$$\psi \equiv \frac{1}{2}(\psi_1 + \psi_2), \qquad \tau \equiv \frac{1}{2}(\psi_1 - \psi_2). \tag{12.37}$$

Then the potential vorticities for each layer may be written as

$$q_1 = \nabla^2\psi + (\nabla^2 - k_d^2)\tau, \qquad q_2 = \nabla^2\psi - (\nabla^2 - k_d^2)\tau, \tag{12.38a,b}$$

and the equations of motion may be rewritten as evolution equations for ψ and τ as follows:

$$\frac{\partial}{\partial t}\nabla^2\psi + J(\psi, \nabla^2\psi) + J(\tau, (\nabla^2 - k_d^2)\tau) = 0, \tag{12.39a}$$

$$\frac{\partial}{\partial t}(\nabla^2 - k_d^2)\tau + J(\tau, \nabla^2\psi) + J(\psi, (\nabla^2 - k_d^2)\tau) = 0. \tag{12.39b}$$

We note the following about the nonlinear interactions in (12.39):

(i) ψ and τ are like vertical modes. That is, ψ is the barotropic mode with a 'vertical wavenumber', k^z, of zero, and τ is a baroclinic mode with an effective vertical wavenumber of one.

(ii) Just as purely two-dimensional turbulence can be considered to be a plethora of interacting triads, whose two-dimensional vector wavenumbers sum to zero, it is clear from (12.39b) that geostrophic turbulence may be considered to be similarly composed of a sum of interacting triads, although now there are two distinct kinds, namely

$$(i) \quad (\psi, \psi) \to \psi, \qquad (ii) \quad (\tau, \tau) \to \psi \quad \text{or} \quad (\psi, \tau) \to \tau. \tag{12.40}$$

The first kind is a *barotropic triad,* for it involves only the barotropic mode. The other two are examples of a *baroclinic triad*. If a barotropic mode has a vertical wavenumber of zero, and a baroclinic mode has a vertical wavenumber of plus or minus one, then the three vertical wavenumbers of the triad interactions must sum to zero. There is no triad that involves only the baroclinic mode, as we may see from the form of (12.39). (If the layers are of unequal depths, then purely baroclinic triads do exist.)

(iii) Wherever the Laplacian operator acts on τ, it is accompanied by $-k_d^2$. That is, it is *as if* the effective horizontal wavenumber (squared) of τ is shifted, so that $k^2 \to k^2 + k_d^2$.

Conservation properties

Multiplying (12.39a) by ψ and (12.39b) by τ and horizontally integrating over the domain of area A, assuming once again that this is either periodic or has solid walls, gives

$$\widehat{T} = \int_A (\nabla\psi)^2 \, dA, \qquad \frac{\mathrm{d}\widehat{T}}{\mathrm{d}t} = \int_A \psi J(\tau, (\nabla^2 - k_d^2)\tau) \,\mathrm{d}A, \tag{12.41a}$$

$$\widehat{C} = \int_A [(\nabla\tau)^2 + k_d^2\tau^2] \,\mathrm{d}A, \qquad \frac{\mathrm{d}\widehat{C}}{\mathrm{d}t} = \int_A \tau J(\psi, (\nabla^2 - k_d^2)\tau) \,\mathrm{d}A. \tag{12.41b}$$

Here, $\widehat{T}$ is the energy associated with the barotropic flow and $\widehat{C}$ is the energy of the baroclinic flow. An integration by parts shows that

$$\int_A \psi J(\tau, (\nabla^2 - k_d^2)\tau)\,\mathrm{d}A = -\int_A \tau J(\psi, (\nabla^2 - k_d^2)\tau)\,\mathrm{d}A, \tag{12.42}$$

and therefore

$$\frac{\mathrm{d}\widehat{E}}{\mathrm{d}t} = \frac{\mathrm{d}}{\mathrm{d}t}(\widehat{T} + \widehat{C}) = 0. \tag{12.43}$$

That is, total energy is conserved.

An enstrophy invariant is obtained by multiplying (12.39a) by $\nabla^2\psi$ and (12.39b) by $(\nabla^2 - k_d^2)\tau$ and integrating over the domain and adding the two expressions. The result is

$$\frac{\mathrm{d}\widehat{Z}}{\mathrm{d}t} = 0, \qquad \widehat{Z} = \int_A (\nabla^2\psi)^2 + \left[(\nabla^2 - k_d^2)\tau\right]^2 \mathrm{d}A. \tag{12.44}$$

This also follows from (12.36).

Just as for two-dimensional turbulence, we may define the spectra of the energy and enstrophy. Then, with obvious notation, for the energy we have

$$\frac{1}{A}\widehat{T} = \int \mathcal{T}(k)\,\mathrm{d}k \quad \text{and} \quad \frac{1}{A}\widehat{C} = \int \mathcal{C}(k)\,\mathrm{d}k. \tag{12.45}$$

The enstrophy spectrum $\mathcal{Z}(k)$ is related to the energy spectra by

$$\frac{1}{A}\widehat{Z} = \int \mathcal{Z}(k)\,\mathrm{d}k = \int \left[k^2\mathcal{T}(k) + (k^2 + k_d^2)\mathcal{C}(k)\right]\,\mathrm{d}k, \tag{12.46}$$

which is analogous to the relationship between energy and enstrophy in two-dimensional flow. We thus begin to suspect that the phenomenology of two-layer turbulence is closely related to, but richer than, that of two-dimensional turbulence.

12.2.3 Phenomenology of Two-layer Turbulence

In this section we explore the phenomenology of two-layer geostrophic turbulence, by examining how the equations of motion simplify if we suppose that the nonlinear interactions occur at particular scales, and by looking at the forms of the triad interactions.

Triad interactions and scales of interactions

Two types of triad interactions are possible:

Barotropic triads. An interaction that is purely barotropic (i.e., as if $\tau = 0$) conserves $\widehat{T}$, the barotropic energy, and the associated enstrophy $\int k^2\mathcal{T}(k)\,\mathrm{d}k$, and a barotropic triad behaves as purely two-dimensional flow. Explicitly, the conserved quantities are

$$\text{energy:} \qquad \frac{\mathrm{d}}{\mathrm{d}t}\Big[\mathcal{T}(k) + \mathcal{T}(p) + \mathcal{T}(q)\Big] = 0, \tag{12.47a}$$

$$\text{enstrophy:} \qquad \frac{\mathrm{d}}{\mathrm{d}t}\left[k^2\mathcal{T}(k) + p^2\mathcal{T}(p) + q^2\mathcal{T}(q)\right] = 0. \tag{12.47b}$$

Baroclinic triads. Baroclinic triads involve two baroclinic wavenumbers (say p, q) interacting with a barotropic wavenumber (say k). The energy and enstrophy conservation laws for this triad are

$$\text{energy:} \qquad \frac{\mathrm{d}}{\mathrm{d}t}\Big[\mathcal{T}(k) + \mathcal{C}(p) + \mathcal{C}(q)\Big] = 0, \tag{12.48a}$$

$$\text{enstrophy:} \qquad \frac{\mathrm{d}}{\mathrm{d}t}\Big[k^2\mathcal{T}(k) + (p^2 + k_d^2)\mathcal{C}(p) + (q^2 + k_d^2)\mathcal{C}(q)\Big] = 0. \tag{12.48b}$$

To the extent that the triad interactions are local, they may be divided into three general types:

(i) interactions only involving scales much smaller than the deformation radius;

(ii) interactions only involving scales much larger than the deformation radius;

(iii) interactions involving scales comparable to the deformation radius.

We consider each in turn.

(i) Interactions at small scales

For small scales the potential vorticity of each layer is given by

$$q_i = \nabla^2\psi_i + \frac{1}{2}k_d^2(\psi_j - \psi_i) \approx \nabla^2\psi_i\,, \tag{12.49}$$

where $i = 1, 2$ and $j = 3 - i$. Thus, each layer is decoupled from the other and obeys the equations of purely two-dimensional turbulence. Enstrophy is cascaded to small scales and, were there to be an energy source at small scales, energy would be transferred upscale until it reached a scale comparable to the deformation scale. As regards triad interactions, interactions at small scales correspond to the case $(p, q) \gg k_d$ in (12.48). If we neglect k_d^2 then we see that a baroclinic triad behaves like a barotropic triad, for (12.48) has the same form as (12.47). In reality, the small scales of a continuously stratified flow may not be representable by a two-layer model, because in a continuously stratified quasi-geostrophic model the enstrophy cascade occurs in *three-dimensional* wavenumber space. Thus, as the horizontal scales become smaller, so does the vertical scale and higher deformation radii (e.g., $n > 1$ in (6.89)) may play a role in reality.

(ii) Interactions at large scales

At scales much larger than the deformation radius we take $|\nabla^2| \sim k^2 \ll k_d^2$, and neglect terms in (12.39) that involve ∇^2 if they appear alongside terms involving k_d^2. Noting that $J(\tau, k_d^2\tau) = 0$, and assuming that $|J(\tau, \nabla^2\psi)| \sim |J(\psi, \nabla^2\tau)|$, we obtain

$$\frac{\partial}{\partial t}\nabla^2\psi + J(\psi, \nabla^2\psi) = -J(\tau, \nabla^2\tau), \qquad \frac{\partial\tau}{\partial t} + J(\psi, \tau) = 0. \tag{12.50a,b}$$

Thus, the baroclinic streamfunction obeys the equation of a passive tracer, although because of the term on the right-hand side of (12.50a) it is not truly passive. Nevertheless, and given the discussion of passive tracers in Section 11.5, these equations suggest that the variance of the baroclinic streamfunction, and thus the energy in the baroclinic mode, will be transferred to smaller scales.

In terms of triad interactions, this case corresponds to $(p, q, k) \ll k_d$. The energy and enstrophy conservation triad interaction laws, (12.48), collapse to

$$\frac{\mathrm{d}}{\mathrm{d}t}\Big[\mathcal{C}(p) + \mathcal{C}(q)\Big] = 0. \tag{12.51}$$

That is to say, energy is conserved among the baroclinic modes alone, with the barotropic mode k mediating the interaction. Consistent with the analysis in physical space, there is no constraint preventing the transfer of baroclinic energy to smaller scales, and no production of barotropic energy at $k \ll k_d$.

(iii) Interactions at scales comparable to the deformation radius

In this case there is, in general, no simplification of the equations in physical space, or of the conservation laws governing triad interactions, and both baroclinic and barotropic modes are important. However, we can write the triad interaction conservation laws in an instructive form if we define

the pseudowavenumber k' by $k'^2 \equiv k^2 + k_d^2$ for a baroclinic mode and $k'^2 \equiv k^2$ for a barotropic mode, and similarly for p' and q'. Then (12.47) and (12.48) can be written as

$$\frac{\mathrm{d}}{\mathrm{d}t}\Big[\mathcal{E}(k) + \mathcal{E}(p) + \mathcal{E}(q)\Big] = 0, \tag{12.52a}$$

$$\frac{\mathrm{d}}{\mathrm{d}t}\Big[k'^2\mathcal{E}(k) + p'^2\mathcal{E}(p) + q'^2\mathcal{E}(q)\Big] = 0, \tag{12.52b}$$

where $\mathcal{E}(k)$ is the energy (barotropic or baroclinic) of the particular mode. These are formally identical with the conservation laws for purely two-dimensional flow and so we expect energy to seek the gravest mode (i.e., smallest pseudowavenumber). Since the gravest mode has $k_d = 0$ this implies a tendency of energy to be transferred into the barotropic mode — a *barotropization* of the flow.

Baroclinic instability in the classic two-layer problem concerns the instability of a flow with vertical but no horizontal shear. This is like a triad interaction for which $p \ll (k, q, k_d)$, where p is the wavenumber of a baroclinic mode, and thus $k^2 \sim q^2$. The triad conservation laws then become

$$\frac{\mathrm{d}}{\mathrm{d}t}\Big[\mathcal{T}(k) + \mathcal{C}(p) + \mathcal{C}(q)\Big] = 0, \tag{12.53a}$$

$$\frac{\mathrm{d}}{\mathrm{d}t}\Big[k^2\mathcal{T}(k) + k_d^2\mathcal{C}(p) + (q^2 + k_d^2)\mathcal{C}(q)\Big] = 0. \tag{12.53b}$$

From these two equations, and with $k^2 \approx q^2$, we derive

$$q^2\dot{\mathcal{C}}(q) = (k_d^2 - k^2)\dot{\mathcal{T}}(k). \tag{12.54}$$

Baroclinic instability requires that both $\dot{\mathcal{C}}(q)$ and $\dot{\mathcal{T}}(k)$ be positive. This can occur only if

$$k^2 < k_d^2. \tag{12.55}$$

Thus, there is a *high-wavenumber cut-off* for baroclinic instability, as we previously found in Section 9.6 by direct calculation. We can see that the cut-off arises by virtue of energy and enstrophy conservation, and is not dependent on linearizing the equations and looking for exponentially growing normal-mode instabilities.

For small scales, we previously noted that each layer is decoupled from the other and that enstrophy, but not energy, may cascade to smaller scales. Now, baroclinic instability (of the large-scale flow) occurs at scales comparable to or larger than the deformation radius. Thus, the energy that is extracted from the mean flow is essentially trapped at scales larger than the deformation scale: it cannot be transferred to smaller scales in a cascade; rather, it is transferred to barotropic flow at scales comparable to the deformation radius, from which it cascades upwards to larger barotropic scales.

Summary of two-layer phenomenology

Putting together the considerations above leads to the following picture of geostrophic turbulence in a two-layer system (Fig. 12.8). At large horizontal scales we imagine some source of baroclinic energy, which in the atmosphere might be the differential heating between pole and equator, or in the ocean might be the wind and surface heat fluxes. Baroclinic instability effects a non-local transfer of energy to the deformation scale, where both baroclinic and barotropic modes are excited. From here there is an enstrophy cascade in each layer to smaller and smaller scales, until eventually the wavenumber is large enough (denoted by k_{3D} in Fig. 12.8) that non-geostrophic effects become important and enstrophy is scattered by three-dimensional effects, and dissipated. At scales larger than the deformation radius, there is an inverse barotropic cascade of energy to larger scales, where

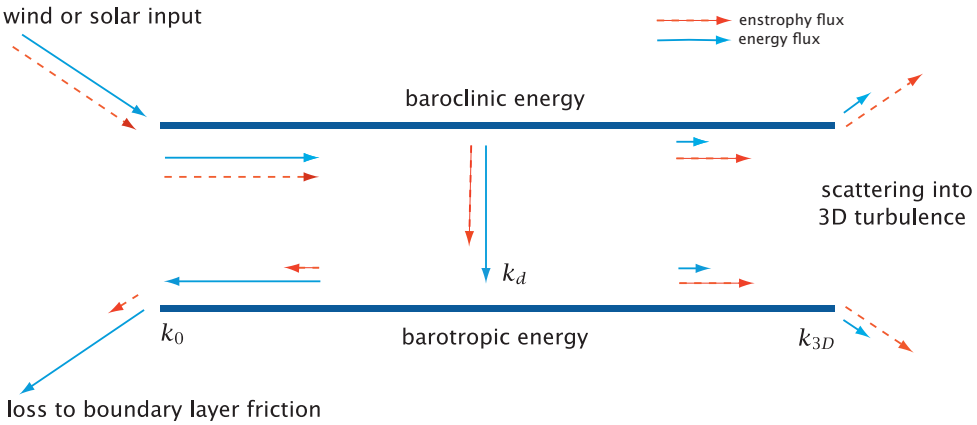

Fig. 12.8 Schema of idealized two-layer baroclinic turbulence.[9] The horizontal axis represents horizontal wavenumber, and the vertical variation is decomposed into two vertical modes — the barotropic and first baroclinic. Energy transfer is shown by solid arrows and enstrophy transfer by dashed arrows.

Large-scale forcing maintains the available potential energy, and so provides energy to the baroclinic mode at very large scales. Energy is transferred to smaller baroclinic scales, and then into barotropic energy at horizontal scales comparable to and larger than the deformation radius (this is baroclinic instability), and then transferred to larger barotropic scales in an upscale cascade. The entire process of baroclinic instability and energy transfer may be thought of as a generalized inverse cascade in which the energy passes to smaller pseudowavenumber $k'^2 \equiv k^2 + k_d^2$.

it is modified by the β-effect and halted by the effects of friction, with the latter being responsible for the dissipation of the large-scale barotropic energy.

There are two aspects of this phenomenology that prevent it from being a quantitative theory of baroclinic eddies in the atmosphere or ocean:

(i) Even as a model of two-layer quasi-geostrophic turbulence the assumptions are questionable. For example, we have largely neglected the effects of friction and we have assumed the baroclinic mode to be passive at large scales. Numerical simulations tend to show a significant transfer of energy from the baroclinic mode to the barotropic mode at scales larger than the deformation radius.

(ii) The ideas do not perfectly apply to either the atmosphere or ocean. In the latter, the turbulence is quite inhomogeneous except perhaps in the Antarctic Circumpolar Current. In the atmosphere, observations indicate that the deformation radius is almost as large as the Rhines scale, and is only a factor-of-a-few smaller than the pole–equator scale, leaving little room for isotropic inverse cascade to fully develop. On the other hand, the atmosphere does display k^{-3} spectra at scales somewhat smaller than the deformation radius (Fig. 12.9), and it may be associated with a forward cascade of enstrophy.[10]

12.3 † A SCALING THEORY FOR GEOSTROPHIC TURBULENCE

Let us now build on the phenomenological model of the previous section and construct a quantitative theory of two-layer forced-dissipative geostrophic turbulence.[12] Although, as we have noted, the underlying model is imperfect, some of its qualitative properties transcend its limitations and are quite revealing about the real system. We will consider a system in which the basic state is a purely zonal flow, with constant vertical shear and no horizontal variation; our goal is to predict the amplitude and the scale of the eddies that result from the baroclinic instability of this flow. The

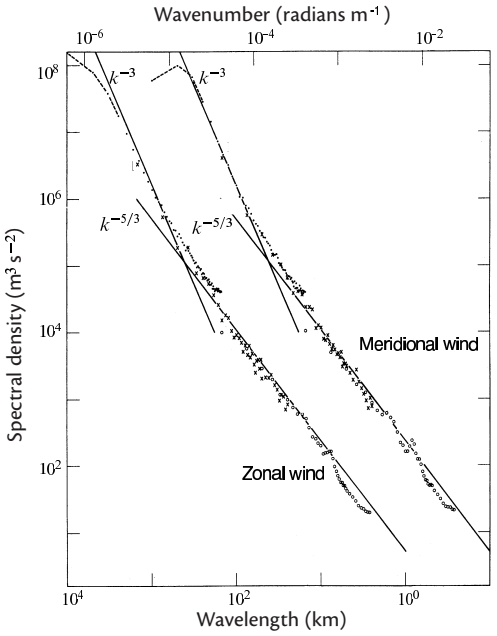

Fig. 12.9 Energy spectra of the zonal and meridional wind near the tropopause, from thousands of commercial aircraft measurements between 1975 and 1979. The meridional spectrum is shifted one decade to the right.

The -3 spectrum may well be associated with a forward enstrophy cascade, but the origin of the $-5/3$ spectrum at smaller scales is not definitively known.[11]

assumptions that the mean flow and the stratification are constants are quite severe and thus the model, even if correct within its own terms of reference, is certainly not a complete theory of the baroclinic eddies in mid-latitude flow.

12.3.1 Preliminaries

We shall suppose that, as in Fig. 12.8, baroclinic instability at large scales leads to a transfer of energy to the barotropic mode at a scale comparable to the deformation radius, followed by an inverse cascade of energy within the barotropic mode, and the energy is finally dissipated in the Ekman layer. At scales smaller than the deformation radius the layers are largely uncoupled, and in each layer there is an enstrophy cascade to small scales. The equations of motion describing all of this are (12.39), but we will explicitly recognize the effect of a shear flow by replacing τ by $\tau - Uy$, where U is constant, this being equivalent to supposing there is a constant shear in the flow. The equations of motion, (12.39), become

$$\frac{\partial}{\partial t}\nabla^2\psi + J(\psi, \nabla^2\psi) + J\big(\tau, (\nabla^2 - k_d^2)\tau\big) + U\frac{\partial}{\partial x}\nabla^2\tau = D_\psi, \tag{12.56a}$$

$$\frac{\partial}{\partial t}(\nabla^2 - k_d^2)\tau + J(\tau, \nabla^2\psi) + J\big(\psi, (\nabla^2 - k_d^2)\tau\big) + U\frac{\partial}{\partial x}(\nabla^2\psi + k_d^2\psi) = D_\tau. \tag{12.56b}$$

These are similar to the equations used for studying two-layer baroclinic instability in Chapter 9, but we now retain the nonlinear terms and include dissipation, represented by D.

For scales much larger than the deformation radius (12.56) become, analogously to (12.50),

$$\frac{\partial}{\partial t}\nabla^2\psi + J(\psi, \nabla^2\psi) = -J(\tau, \nabla^2\tau) - U\frac{\partial}{\partial x}\nabla^2\tau + D_\psi, \tag{12.57}$$

$$\frac{\partial\tau}{\partial t} + J(\psi, \tau) = U\frac{\partial\psi}{\partial x} - k_d^{-2}D_\tau]. \tag{12.58}$$

The equation for ψ is just the barotropic vorticity equation, 'forced' via its interaction with the baroclinic mode, namely the terms on the right-hand side of (12.57). The equation for the baro-

clinic streamfunction is the same as the equation for a passive scalar, except for the forcing term $U\partial\psi/\partial x$.

12.3.2 Scaling Properties

In the barotropic equation, we may argue that in the energy-containing scales, $k^2 \ll k_d^2$, the magnitude of the barotropic streamfunction is much larger than that of the baroclinic streamfunction; that is, $|\psi| \gg |\tau|$, as follows. We may reasonably suppose that the forcing of the barotropic vorticity equation occurs at wavenumbers close to k_d, as in baroclinic instability. At larger scales the barotropic streamfunction obeys the two-dimensional vorticity equation, and we may expect an energy cascade to large scales with energy spectrum given by

$$\mathcal{E}_\psi(k) = \mathcal{K}_1 \varepsilon^{2/3} k^{-5/3}, \tag{12.59}$$

where $\mathcal{K}_1$ is a constant and ε is the as yet undetermined energy flux through the system. We may suppose that this cascade holds for wavenumbers $k_0 < k \ll k_d$, where the wavenumber k_0 is the halting scale of the inverse cascade, determined by one or more of: friction, the β-effect, and the domain size. Now, in this same wavenumber regime the baroclinic streamfunction is being advected as a passive tracer — it is being stirred by ψ. Thus, any baroclinic energy that is put in at large scales by the interaction with the mean flow (via the term proportional to $U\psi_x$) will be cascaded to smaller scales. Thus, we expect the baroclinic energy spectrum to be that of a passive tracer whose variance is cascading to smaller scales in a forward cascade, with a spectrum given by (cf. (11.92))

$$\mathcal{E}_\tau(k) = \mathcal{K}_2 \varepsilon_\tau \varepsilon^{-1/3} k^{-5/3}, \tag{12.60}$$

where $\mathcal{K}_2$ is a constant, ε_τ is the transfer rate of baroclinic energy and ε is the same quantity appearing in (12.59). Now, because energy is not lost to small scales we have $\varepsilon_\tau = \varepsilon$, both being equal to the energy flux in the system. Thus, using (12.59) and (12.60), the energy in the barotropic and baroclinic modes is comparable at sufficiently large scales. Since the energy density in the former is $(\nabla\psi)^2$ and in the latter $(\nabla\tau)^2 + k_d^2\tau^2 \sim k_d^2\tau^2$, the magnitude of ψ must then be much larger than that of τ, and specifically

$$|\psi| \sim \frac{k_d|\tau|}{k_0} \gg |\tau|. \tag{12.61}$$

Let us write the baroclinic equation (12.58) in the form

$$\frac{\partial\tau}{\partial t} + J(\psi, \tau - Uy) = 0, \tag{12.62}$$

which is the equation for a passive tracer (τ) in a mean gradient (U), stirred by the flow (ψ), and we omit dissipation. Because there is a large scale separation (in fact, an infinite one) between the scale of the mean gradient of τ (i.e., the scale of variations of U) and the scale of its fluctuations, we can write

$$\tau \sim l' \frac{\partial\overline{\tau}}{\partial y} = -l'U, \tag{12.63}$$

where l' is the scale of the fluctuation. Thus, at the scale k_0^{-1}, the magnitude of τ, and the associated baroclinic velocity v_τ, are given by

$$\tau \sim \frac{U}{k_0}, \qquad v_\tau \sim U. \tag{12.64}$$

At this scale, and using (12.61), the magnitude of the barotropic streamfunction and its associated velocity are given by

$$\psi \sim \frac{k_d U}{k_0^2}, \qquad v_\psi \sim \frac{k_d U}{k_0}. \tag{12.65a,b}$$

This is an important result, regardless of the other details in the calculation. In particular, (12.65b) implies that the barotropic velocity, v_ψ, scales like the mean velocity U multiplied by the ratio of the length scale of the eddies to the deformation radius. In the Earth's atmosphere, this ratio is an $\mathcal{O}(1)$ number; in the ocean it is somewhat larger.

How much energy flows through the system? The mean shear is the ultimate source of energy, and for simplicity this shear is kept constant in time, analogous to an infinite heat bath supplying energy to a smaller system without its own temperature changing. The conversion of energy from the mean shear to the eddy flow is given by multiplying (12.58) by $k_d^2\tau$ and integrating over the domain. This gives an expression for the rate of increase of the available potential energy of the system, namely

$$\frac{\mathrm{d}}{\mathrm{d}t}\mathrm{APE} = \frac{\mathrm{d}}{\mathrm{d}t}\int_A k_d^2\tau^2\,\mathrm{d}A = \int_A 2Uk_d^2\tau\frac{\partial\psi}{\partial x}\,\mathrm{d}A. \tag{12.66}$$

(Note that the energy input to the system equals the poleward heat flux.) From this we estimate the average energy flux as

$$\varepsilon = 2Uk_d^2\overline{\psi_x\tau} \sim \frac{U^3k_d^3}{k_0^2}. \tag{12.67}$$

The correlation between ψ_x and τ cannot be determined by this argument. This aside, we have produced a physically based closure for the flux of energy through the system in terms only of the mean shear, the halting scale k_0 (discussed below) and the deformation scale k_d.

Finally, we calculate the eddy diffusivity (considered at greater length in chapter 13),

$$\kappa \equiv -\frac{\overline{v_\psi\tau}}{\partial_y\overline{\tau}} = \kappa \sim \frac{k_dU}{k_0^2}, \tag{12.68}$$

using (12.64) and (12.65). If the mixing velocity is the barotropic stirring velocity, this result implies a mixing length of k_0^{-1} and that the eddy diffusivity is just the magnitude of the barotropic streamfunction at the energy-containing scales.

12.3.3 The Halting Scale and the β Effect

Let us suppose that, as discussed in Section 12.1, the β effect provides a barrier for the inverse cascade at the scale (12.11), so that $k_0 = k_\varepsilon \sim (\beta^3/\varepsilon)^{1/5}$. Using (12.67) we find that the stopping scale is given by

$$k_0 = k_\varepsilon \sim \frac{\beta}{Uk_d}, \tag{12.69}$$

and using (12.68) and (12.69) we obtain for the energy flux and the eddy diffusivity,

$$\varepsilon \sim \frac{U^5k_d^5}{\beta^2}, \qquad \kappa \sim \frac{U^3k_d^3}{\beta^2}. \tag{12.70}$$

The magnitudes of the eddies themselves are easily given using (12.65) and (12.64), whence

$$\tau \sim \frac{U^2k_d}{\beta}, \quad v_\tau \sim U, \qquad \psi \sim \frac{U^3k_d^3}{\beta^2}, \quad v_\psi \sim \frac{U^2k_d^2}{\beta}. \tag{12.71}$$

Evidently, in this model (in which the mean shear and deformation radius are fixed), the eddies become more energetic with decreasing β, and the eddy amplitudes and poleward heat flux increase very rapidly with the mean shear, more so than in a model in which the energy-containing scale is fixed. This is because as β decreases, the inverse cascade can extend to larger scales, thereby increasing the overall energy of the flow. Similarly, as U increases not only does the eddy amplitude increase as a direct consequence, as in (12.64) and (12.65), but also k_ε falls (see (12.69)), and these effects combine to give a rapid increase of the eddy magnitudes with U.

Frictional effects

Whether β is present or not, friction is necessary to ultimately remove the energy flowing through the system, as well as to remove enstrophy at small scales. Friction provides another mechanism for halting the inverse cascade, and the simplest case is that of a linear drag representing Ekman friction, in which case we write

$$D_\psi = -r\nabla^2\psi. \tag{12.72}$$

and the stopping wavenumber for a given ε is given, as in (11.68), by $k_r = (r^3/\varepsilon)^{1/2}$. However, a little algebra shows that the use of this in (12.67) fails to give a result for ε. From a physical perspective, a linear drag that is weak enough to allow an inverse cascade to form is, *ipso facto,* too weak to equilibrate the flow. A friction that becomes larger at larger scales, for example an 'inverse Laplacian', has no such problems. More physically, a nonlinear drag, proportional to the square of the amplitude of the flow, also leads to a well-posed problem with the cascade halting at a well-defined scale. Finally, we should point out that in neither the atmosphere nor ocean is there an extended inverse cascade, because the deformation scale and the beta scale are not asymptotically well separated (although the β-effect does not prevent an inverse cascade to large zonal scales).

12.4 † PHENOMENOLOGY OF BAROCLINIC EDDIES IN THE ATMOSPHERE AND OCEAN

In the remaining sections of this chapter we take a more informal approach, illustrated by numerical experiments, to the problem of baroclinic eddies in the atmosphere and ocean. We draw from our treatment of geostrophic turbulence but by being a little less formal we are able to travel farther, for we spend less time looking at the map (but with a concomitant danger that we lose our way).

12.4.1 The Magnitude and Scale of Baroclinic Eddies

How big, in both amplitude and scale, do baroclinic eddies become? Suppose that the time-mean flow is given, and that it is baroclinically unstable. Eddies will grow, initially according to the linear theory of Chapter 9, but they cannot and do not continue to amplify: they ultimately equilibrate, and this by way of nonlinear mechanisms. The eddies will extract energy from the mean flow, but at the same time the available energy of the mean flow is being replenished by external forcing (i.e., the maintenance of an equator–pole temperature gradient by radiative forcing in the atmosphere, and wind and buoyancy forcing at the surface in the ocean). Thus, we cannot a priori determine the amplitude of baroclinic eddies by simply assuming that all of the available potential energy in the mean flow is converted to eddying motion. To close the problem we find we need to make three, not necessarily independent, assumptions:

(i) an assumption about the magnitude of the baroclinic eddies;

(ii) an assumption relating eddy kinetic energy to eddy available potential energy;

(iii) an assumption about the horizontal scale of the eddies.

Baroclinic eddies extract available potential energy (APE) from the mean flow, and it is reasonable to suppose that an eddy of horizontal scale L_e can extract, as an upper bound, the APE of the mean flow contained within that scale. The APE is proportional to the variation of the buoyancy field so that

$$(\Delta b')^2 \sim |\Delta\bar{b}|^2 \sim L_e^2|\nabla\bar{b}|^2, \tag{12.73}$$

where Δb is the variation in the buoyancy over the horizontal scale L_e. (For simplicity we stay with the Boussinesq equations, and $b = -g\delta\rho/\rho_0$. We could extend the arguments to an ideal-gas atmosphere with $b = g\delta\theta/\theta_0$.) Equivalently, we might simply write

$$b' \sim L_e|\nabla\bar{b}|, \tag{12.74}$$

which arises from a mixing-length approach. Supposing that the temperature gradient is mainly in the y-direction then, using thermal wind, we have

$$b' \sim L_e f \frac{\partial \overline{u}}{\partial z} \qquad \text{and} \qquad v'_\tau \sim \overline{u}, \tag{12.75a,b}$$

where v'_τ is an estimate of the shear (multiplied by the depth scale) of the eddying flow. (These estimates are the same as (12.64), with $\overline{u}$ replacing U.)

Our second assumption is to relate the barotropic eddy kinetic energy to the eddy available potential energy, and the most straightforward one to make is that there is a rough equipartition between the two. This assumption is reasonable because in the baroclinic lifecycle (or baroclinic inverse cascade) energy is continuously transferred from eddy available potential energy to eddy kinetic energy, and the assumption is then equivalent to supposing that the relevant eddy magnitude is always proportional to this rate of transfer. Thus we assume $v'^2_\psi \sim (b'/N)^2$ or

$$v'_\psi \sim \frac{b'}{N}. \tag{12.76}$$

Finally, the scale of the eddies is determined by the extent to which the eddies might grow through nonlinear interactions. As we discussed earlier, possibilities for this scale include the deformation radius itself (if the inverse cascade is weak) or the Rhines scale (if the inverse cascade is slowed by the β-effect), or even the domain scale if neither of these applies.

Some consequences

The simple manipulations above have some very interesting consequences. Using (12.75) and (12.76) we find

$$v'_\psi \sim \frac{f L_e}{NH}\overline{u} = \frac{L_e}{L_d}\overline{u}, \tag{12.77}$$

where $L_d = NH/f_0$ is the deformation radius and $\overline{u}$ is the amplitude of the mean baroclinic velocity, that is the mean shear multiplied by the height scale. This important relationship relates the magnitude of the eddy kinetic energy to that of the mean. In the atmosphere the scale of the motion is not much larger than the deformation radius (which is about 1000 km) and the eddy and mean kinetic energies are, consistently, comparable to each other. In the ocean the deformation radius (about 50 km over large areas) is significantly smaller than the scale of mesoscale eddies (which is more like 200 km or more), and observations consistently reveal that the eddy kinetic energy is an order of magnitude larger than the mean kinetic energy.[13]

One other important and slightly counter-intuitive result concerns the timescale of eddies. From (12.77) we have

$$T_e \sim \frac{L_e}{v'_\psi} \sim \frac{L_d}{\overline{u}} \equiv T_E, \tag{12.78}$$

where T_E is the Eady time scale. That is, the eddy time scale (at the scale of the largest eddies) is independent of the process that ultimately determines the spatial scale of those eddies; if the eddy length scale increases somehow, perhaps because friction or β are decreased, the velocity scale increases in proportion.

12.4.2 Baroclinic Eddies and their Lifecycle in the Atmosphere

Amplitude and scale

We saw in Section 9.9.2 that baroclinic instability in the atmosphere occurs predominantly in the troposphere, i.e., in the lowest 10 km or so of the atmosphere, with the higher stratification of the

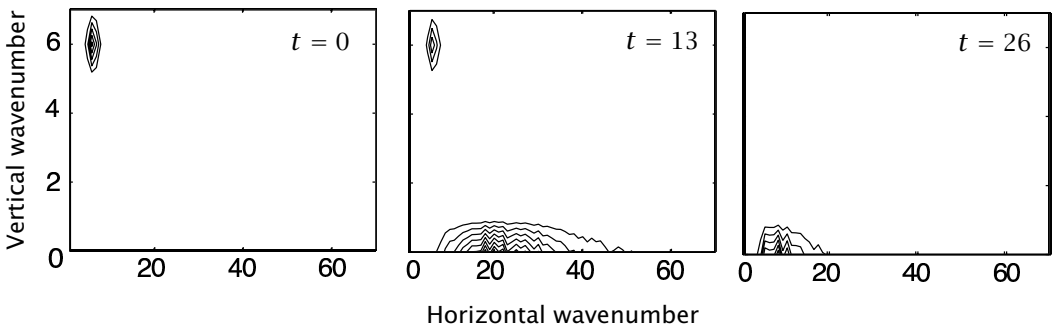

Fig. 12.10 A numerical simulation of an idealized baroclinic lifecycle, showing contours of energy in spectral space at successive times. Initially, there is baroclinic energy at low horizontal wavenumber, as in a large-scale shear. Baroclinic instability transfers this energy to barotropic flow at the scale of the deformation radius, and this is followed by a barotropic inverse cascade to large scales. Most of the transfer to the barotropic mode in fact occurs quite quickly, between times 11 and 14, but the ensuing barotropic inverse cascade is slower. The entire process may be thought of as a generalized inverse cascade. The stratification (N^2) is uniform, and the first deformation radius is at about wavenumber 15. Times are in units of the eddy turnover time.[15]

eponymous stratosphere inhibiting instability. In the mid-latitude troposphere the vertical shear and the stratification are relatively uniform and fairly simple models, such as the two-layer model or the Eady model (with the addition of the β-effect) are reasonable first-order models.

The mean pole–equator temperature gradient is about 40 K and the deformation radius NH/f is about 1000 km. The Rhines scale, $\sqrt{U/\beta}$ is a little larger than the deformation radius, being perhaps 2000 km, and is similar to the width of the main mid-latitude baroclinic zone which lies between about 40° and 65°, in either hemisphere. Given these, and especially given that the maximum wavelength for instability occurs at scales somewhat larger than the deformation radius, there is little prospect of an extended upscale cascade, and for this reason the Earth's atmosphere has comparable eddy kinetic and mean kinetic energies.[14]

The baroclinic lifecycle

The baroclinic lifecycle of geostrophic turbulence, sketched schematically in Fig. 12.8, can be nicely illustrated by way of numerical initial value problems, and we describe two such. The first is extremely idealized: take a doubly-periodic quasi-geostrophic model on the f-plane, initialize it with baroclinic energy at large horizontal scales, and then let the flow freely evolve. Figure 12.10 shows the results. The flow, initially concentrated in high vertical wavenumbers to best illustrate the energy transfer, is baroclinically unstable, and energy is transferred to barotropic flow at wavenumbers close to the first radius of deformation, here at about wavenumber 15. Energy then slowly cascades back to large scales in a predominantly barotropic inverse cascade, piling up at the largest scales much as in decaying, two-dimensional turbulence. Nearly all of the initial baroclinic energy is converted to barotropic, eddy kinetic energy and, even without any surface friction, the flow evolves to a baroclinically stable state. Couched in these terms, it is easy to see that the baroclinic lifecycle is a form of baroclinic inverse cascade, with an energy transfer to large total wavenumber, K_{tot}, that is made up of contributions from both horizontal and vertical wavenumbers:

$$K_{tot}^2 = K_h^2 + k_d^2 m^2, \tag{12.79}$$

where m is the vertical wavenumber and K_h is the horizontal wavenumber. As we noted earlier, the twin constraints of energy and enstrophy conservation prevent the excitation of horizontal scales with very large horizontal wavenumbers, and so the lifecycle proceeds through wavenumbers at the deformation scale.

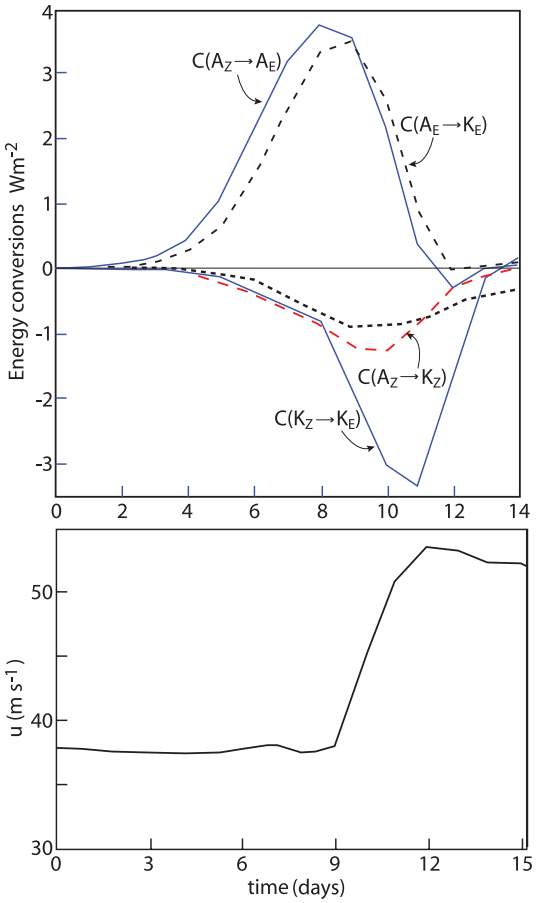

Fig. 12.11 Top: energy conversion and dissipation processes in a numerical simulation of an idealized atmospheric baroclinic lifecycle, simulated with a GCM. Bottom: evolution of the maximum zonal-mean velocity. Top: energy conversions. A_Z and A_E are zonal and eddy available potential energies (APEs), and K_Z and K_E are the corresponding kinetic energies, and $C(\cdot \rightarrow \cdot)$ represents the corresponding conversion.

Initially baroclinic processes dominate, with conversions from zonal to eddy APE, $C(A_Z \rightarrow A_E)$, and then eddy APE to eddy kinetic energy, $C(A_E \rightarrow K_E)$, followed by the barotropic conversion of eddy kinetic to zonal kinetic energy, a negative value of $C(K_Z \rightarrow K_E)$. The latter process is reflected in the *increase* of the maximum zonal-mean velocity at about day 10, shown in the lower panel.[16]

The results of the second, and more realistic, initial value problem are illustrated in Fig. 12.11. Here, the atmospheric primitive equations on a sphere are integrated forward, beginning from a baroclinically unstable zonal flow, plus a small-amplitude disturbance at zonal wavenumber 6. The disturbance grows rapidly through baroclinic instability, accompanied by a conversion of energy initially from the zonal mean potential energy to eddy available potential energy (EAPE), and then from EAPE to eddy kinetic energy (EKE), and finally from EKE to zonal kinetic energy (ZKE). The last stage of this roughly corresponds to the barotropic inverse cascade of quasi-geostrophic theory, and because of the presence of a β-effect the flow becomes organized into a zonal jet. The parameters in the Earth's atmosphere are such that there is only one such jet, and in the lower panel of Fig. 12.11 we see its amplitude increase quickly from days 10 to 12, associated with the conversion of EKE to ZKE. (In other lifecycle experiments, the end state is found to be more akin to a barotropic vortex or, in meteorological parlance, a 'cut-off cyclone'.[17]) A commonality between all the lifecycles is the evolution toward a generally barotropic flow, with variable degrees of zonality in the final state, depending on the importance of the β-effect.

Of course, the real atmosphere is never in the zonally uniform state that is used in idealized baroclinic instability or lifecycle studies. Rather, at any given time, finite-amplitude eddies exist and these provide a finite amplitude perturbation to the baroclinically unstable zonal flow. For this reason we rarely, if ever, see an exponentially growing normal mode. Furthermore, given any instantaneous atmospheric state, zonally symmetric or otherwise, the fastest growing (linear) instability is not necessarily exponential but may be 'non-modal', with a secular or linear growth that, over some finite time period and in some given norm, is much more rapid than exponential.[18]

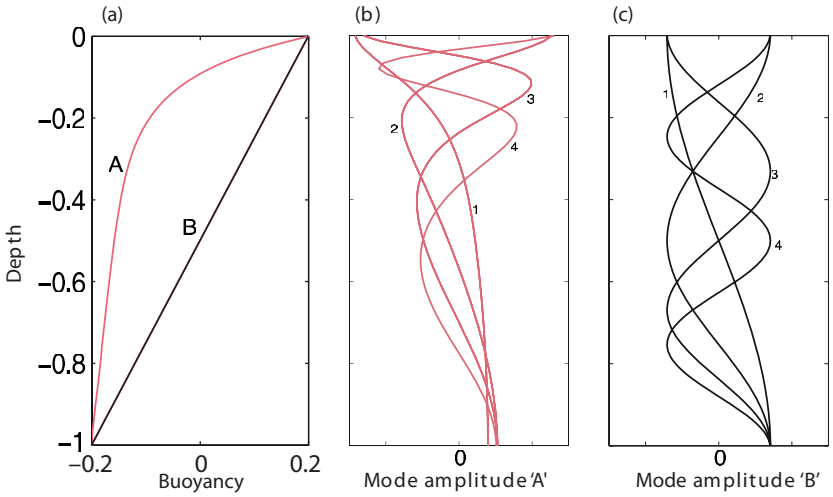

Fig. 12.12 (a) Two buoyancy profiles, $-g\delta\rho/\rho_0$, one being a fairly realistic oceanic case with enhanced stratification in the upper ocean (profile A), and the other with uniform stratification (profile B). (b) and (c) The first four baroclinic modes [eigenfunctions of (12.80)] for A and B. With profile B the eigenmodes are cosines, whereas in profile A they have a larger amplitude and shorter local wavelength in the upper ocean. The number of zero crossings is equal to the mode number.

12.4.3 Baroclinic Eddies and their Lifecycle in the Ocean

Basic ideas

Baroclinic instability was first developed as a theory for mid-latitude instabilities in the atmosphere and the original problems were set in a zonally re-entrant channel. The ocean, apart from the Antarctic Circumpolar Current (ACC), is not zonally re-entrant. However, it is driven by buoyancy and wind-forcing at the surface, and these combine to produce a region of enhanced stratification and associated shear in the ocean in the upper 500–1000 m or so — that is, in the 'thermocline' — as discussed more fully in Chapter 20. The associated sloping isopycnals constitute a pool of available potential energy, and so the ocean is potentially baroclinically unstable. Satellite observations indicate that baroclinic eddies are in fact almost ubiquitous in the mid- and high-latitude oceans, especially in and around intense western boundary currents, such as the Gulf Stream, and the ACC. The ocean is, literally, a sea of eddies.[19]

In addition to the geometry, the main differences between the oceanic and atmospheric problems are twofold:

(i) In the ocean, the shear and the stratification are not uniform between two rigid lids, nor even uniform between one rigid lid and a structure like the tropopause. Instead, both stratification and shear are largest in the upper ocean, decaying into a quiescent and nearly unstratified abyss.

(ii) In the ocean, the first radius of deformation is much smaller than the scale of the large-scale flow; that is, of the gyres or the large-scale overturning circulation. On dimensional grounds we have, using a height scale and stratification representative of the upper ocean, $L_d \sim NH/f \sim 10^{-2} \times 10^3/10^{-4} = 100\,\text{km}$.

A consequence of the enhanced shear in the upper ocean is that the amplitude of the growing waves is also largely concentrated in the upper ocean, as we saw in Fig. 9.22. Regarding the stratification, in quasi-geostrophic theory we may, as in Section 6.5.2, define the deformation radii by

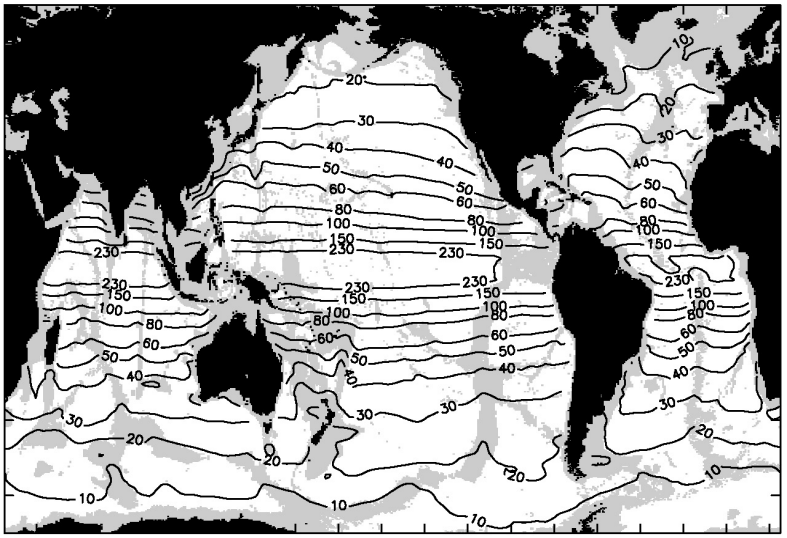

Fig. 12.13 The oceanic first deformation radius L_d in kilometres, calculated using the observed stratification and an equation similar to (12.80). Near equatorial regions are excluded, and regions of ocean shallower than 3500 m are shaded.

Variations in Coriolis parameter are responsible for much of large-scale variability, although weak stratification also reduces the deformation radius at high latitudes.[21]

solution of the eigenvalue problem

$$\frac{\partial}{\partial z}\frac{f^2}{N^2}\frac{\partial \phi_n}{\partial z} + \Gamma_n \phi_n = 0, \qquad \text{with} \qquad \frac{\partial \phi_n}{\partial z} = 0 \quad \text{at } z = 0,\ H. \tag{12.80a,b}$$

The successive eigenvalues, Γ_n, are related to the successive deformation radii, L_n, by $L_n^2 = 1/\Gamma_n$. If the stratification (N^2) is uniform the resulting eigenfunctions are cosines with corresponding eigenvalues and deformation radii given by

$$\Gamma_n = n^2 \frac{f^2 \pi^2}{N^2 H^2}, \qquad L_n = \frac{1}{\sqrt{\Gamma_n}} = \frac{NH}{n\pi f_0}. \tag{12.81a,b}$$

If the stratification is non-uniform, we must in most cases solve the eigenproblem numerically (or by WKB methods, see Section 3.4.2), and the results of one such calculation are given in Fig. 12.12. The case with uniform stratification reproduces cosine modes, whereas in the more realistic case the modes tend to have highest amplitude in the upper ocean, where the stratification is strongest — a result that is typical of oceanic profiles.[20]

The results of a calculation of the first deformation radius using observed oceanic profiles are given in Fig. 12.13, and values of 50–100 km emerge in mid-latitudes.[22] We may therefore expect oceanic baroclinic instability to occur on a scale much smaller than that in the atmosphere, and much smaller than the scale of an ocean basin. (However, the scale of baroclinic instability will typically be larger than the first deformation radius, L_1, shown in Fig. 12.13, because of two compounding effects. First, in uniform stratification the first deformation radius, L_1, as given by (12.81b) is a factor of π smaller than the simple definition NH/f. Second, in simple baroclinic instability problems like the Eady problem the wavelength of maximum instability is a few times NH/f. Thus, the wavelength of maximum instability may be an order of magnitude larger than L_1.)

Eddy amplitudes and scales

The consequences of this small deformation radius on the lifecycle and finite-amplitude equilibration of oceanic baroclinic eddies are far-reaching, one being that there is more scope for an inverse cascade than in the atmosphere, and indeed observations indicate that the horizontal scale of the

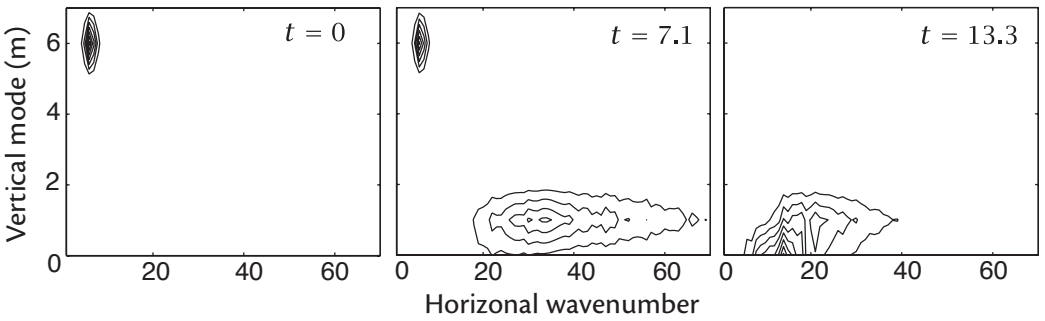

Fig. 12.14 Idealized baroclinic lifecycle, similar to that in Fig. 12.10, but with enhanced stratification of the basic state in the upper domain, representing the oceanic thermocline.

eddies is typically a few to several times larger than the local deformation radius itself. The situation is not clear cut, however, as some observations[23] indicate that the eddy size nevertheless scales with the local deformation radius, suggesting that the eddy scale may be set by the instability scale and not an inverse cascade.

In any case, suppose that an ocean eddy has a horizontal scale 200 km, and that it sits in the subtropical gyre where the mean temperature gradient is $10^{-5}\,\mathrm{K\,m^{-1}}$, that the mean shear and ensuing baroclinic activity are mainly confined to the upper 1000 m of the ocean, and that the deformation radius is 50 km. The temperature gradient corresponds to a temperature difference of about 20 K across 2000 km, a horizontal buoyancy gradient of about $2\times10^{-9}\,\mathrm{s^{-2}}$ [using the simple equation of state $\rho=\rho(1-\beta_T\Delta T)$ where $\beta_T=2\times10^{-4}\,\mathrm{K^{-1}}$] and a shear of about $2\,\mathrm{cm\,s^{-1}}$ over the upper 1 km of ocean. Then, using (12.77), we can estimate a typical eddy velocity scale as

$$v'_\psi \sim \frac{L_e}{L_d}\overline{u} \approx 4\overline{u} \approx 8\,\mathrm{cm\,s^{-1}}, \tag{12.82}$$

implying, as we noted earlier, an EKE that is an order of magnitude larger than the mean kinetic energy. Associated with this are typical temperature perturbations whose magnitude we can estimate using (12.74) or (12.75) as being about 2 K. These estimates are comparable to those observed in mid-ocean, with more energetic eddies forming near intense western boundary currents where gradients are large and barotropic instability also provides a source of energy for the eddies. There is least a factor-of-a-few uncertainty, but it is noteworthy that they are roughly comparable to the values observed.

Eddy lifecycles

The lifecycle of a mid-oceanic baroclinic eddy will differ from its atmospheric counterpart in two main respects:

(i) Baroclinic eddies may be advected by the mean flow into regions with quite different properties from where they initially formed.

(ii) The non-uniformity of the stratification affects the passage to barotropic flow.

Both of these can best be studied by numerical means. Regarding the first, eddies will often form in or near intense western boundary currents, but then will be advected by that current into the potentially less unstable open ocean before completing their lifecycle. Regarding the second, an oceanic analogue of the lifecycle illustrated in Fig. 12.10 is shown in Fig. 12.14. The main difference between this case and the atmospheric one is that baroclinic instability initially leads to the transfer of energy to vertical mode one, followed by a transfer to larger horizontal scales in the barotropic mode, as illustrated schematically in Fig. 12.15.[24] If the energy is initially solely in the

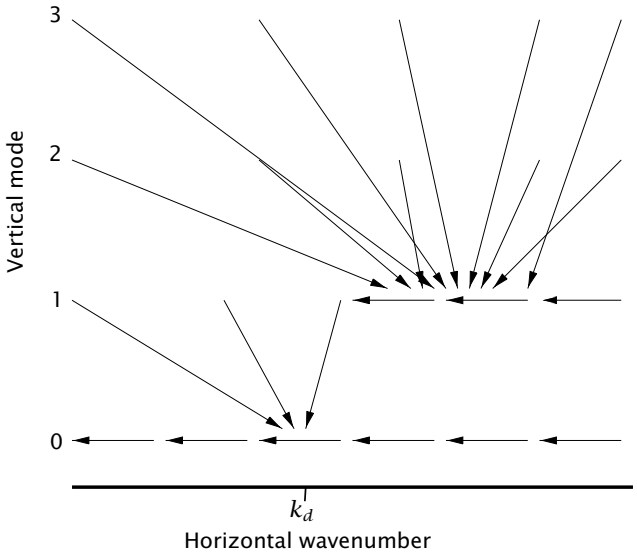

Fig. 12.15 Energy transfer paths as a function of vertical mode and horizontal wavenumber, in a fluid with an oceanic stratification; i.e., with a thermocline. Vertical mode 0 is the barotropic mode.

first baroclinic mode the cycle is more similar to the atmospheric one, but higher baroclinic modes may be more readily excited in the ocean than the atmosphere.

Notes

1 Rhines (1975). See also Holloway & Hendershott (1977) and Vallis & Maltrud (1993).

2 Adapted from Vallis & Maltrud (1993).

3 The mechanism described here follows Vallis & Maltrud (1993). Interactions between Rossby waves will also give rise to zonal flow, as described by Newell (1969) and Rhines (1975). Wave–mean-flow interactions provide a direct route to the production of zonal flows, as discussed in Chapter 15. Williams (1978) was one of the first numerical simulations to show the production of jets.

4 More discussion on these matters is variously given by Smith *et al.* (2002), Danilov & Gryanik (2002), Galperin *et al.* (2006, 2010), Sukoriansky *et al.* (2007), Scott & Dritschel (2012), Chai (2016) and others.

5 A PV staircase was proposed for the jets of Jupiter by Marcus (1993) and further discussed by Peltier & Stuhne (2002), and a review is to be found in Dritschel & McIntyre (2008). Staircases in turbulent flow can and have been found more generally, in particular in stratified flow in which an initially smooth density gradient may break down into steps and layers when stirred (Phillips 1972, Ruddick *et al.* 1989).

6 Adapted from Scott & Dritschel (2012).

7 Farrell & Ioannou (1995, 2008) and Srinivasan & Young (2012) describe a direct pathway to zonal jets that does not require eddy–eddy interactions. Tobias & Marston (2013) describe the mechanisms in a more general context at the price of some analytic accessibility, discussing the circumstances in which the jet formation proceeds by way of a cascade or a direct interaction with the zonal flow.

8 Quasi-geostrophic turbulence was introduced by Charney (1971). Salmon (1980) and Rhines (1977) provided much of the two-layer phenomenology. Various laboratory experiments are discussed by Read (2001).

9 Adapted from Salmon (1980).

10 Lindborg (1999) concluded that the data were consistent with a forward cascade of enstrophy between wavelengths of a few thousand kilometres and a few hundred kilometres. Boer & Shepherd

(1983) and Shepherd (1987) also found a k^{-3} spectrum at similar scales, noting the importance of interactions involving stationary waves. At scales smaller than than 100 km or so the spectrum is shallower than -3, and more like $-5/3$. This may be due to non-geostrophic effects, for example a forward cascade of energy associated with gravity wave breaking, or it may be due to a two-dimensional inverse cascade of energy with an energy source at very small scales associated with convection, or it may be due to effects associated with 'surface quasi-geostrophic' dynamics.

11 Adapted from Gage & Nastrom (1986).

12 Larichev & Held (1995) and Held & Larichev (1996). See Spall (2000) for an oceanic extension, and Thompson & Young (2006) for evidence that the theory fails to account for coherent structures.

13 Related arguments concerning eddy magnitudes were given by Gill *et al.* (1974). Atmospheric energetics, and atmospheric observations in general, are described by Peixoto & Oort (1992). For the oceanic case, see Wyrtki *et al.* (1976), Richardson (1983), and Stammer (1997).

14 This does not address the issue as to *why* the Rhines scale and deformation radius are similar. See also Chapter 15.

15 Modified from Smith & Vallis (2001).

16 Adapted from Simmons & Hoskins (1978).

17 See Thorncroft *et al.* (1993). These authors identify two classes of lifecycles, which they call LC1 and LC2, which have differing degrees of decay of eddy kinetic energy in the later parts of the lifecycle, and with LC2 producing cut-off cyclones. Initial conditions and spatial inhomogeneities, including the horizontal shear of the flow and the presence of critical layers, play an important role in guiding the location of the wave breaking, and hence the final state that is reached.

18 The theory of this as applied to the atmosphere has been developed by Farrell (1984), Farrell & Ioannou (1996) and other papers by these authors. Exponential growth is the exception, not the rule, in baroclinic instability in the real world, both because of nonlinear effects and non-normal instabilities. Indeed, if the basic flow is oscillatory, baroclinic instability can arise even if the basic flow is never unstable via the CSP criterion.

19 This realization came to fruition as a result of the bilateral US–USSR POLYMODE project in the 1970s. See Robinson (1984).

20 For example, Kundu *et al.* (1975).

21 From Chelton *et al.* (1998).

22 The eigenproblem actually solved was

$$\partial^2\phi/\partial z^2 + (N^2(z)/c^2)\phi = 0, \qquad \phi = 0 \quad \text{at } z = 0, H, \tag{12.83}$$

where H is the ocean depth and N is the observed buoyancy frequency. The deformation radius is given by $L_d = c/f$ where c is the first eigenvalue and f is the latitudinally varying Coriolis parameter.

23 Stammer (1997).

24 Fu & Flierl (1980) and Smith & Vallis (2001) examined this issue in more detail, both analytically and numerically. Figure 12.15 is adapted from these papers.